PROCEEDINGS OF SPIE

SPIEDigitalLibrary.org/conference-proceedings-of-spie

"Cut-and-paste" manufacture of multiparametric epidermal electronic systems

Nanshu Lu
Shixuan Yang
Pulin Wang

SPIE.

"Cut-and-Paste" Manufacture of Multiparametric Epidermal Electronic Systems

Nanshu Lu[*abc], Shixuan Yang[a], Pulin Wang[a]
[a]Center for Mechanics of Solids, Structures and Materials, Department of Aerospace Engineering and Engineering Mechanics, [b]Texas Materials Institute, [c]Department of Biomedical Engineering, the University of Texas at Austin, Austin TX 78712, USA.

ABSTRACT

Epidermal electronics is a class of noninvasive and unobstructive skin-mounted, tattoo-like sensors and electronics capable of vital sign monitoring and establishing human-machine interface. The high cost of manpower, materials, vacuum equipment, and photolithographic facilities associated with its manufacture greatly hinders the widespread use of disposable epidermal electronics. Here we report a cost and time effective, completely dry, benchtop "cut-and-paste" method for the freeform and portable manufacture of multiparametric epidermal sensor systems (ESS) within minutes. This versatile method works for all types of thin metal and polymeric sheets and is compatible with any tattoo adhesives or medical tapes. The resulting ESS are multimaterial and multifunctional and have been demonstrated to noninvasively but accurately measure electrophysiological signals, skin temperature, skin hydration, as well as respiratory rate. In addition, planar stretchable coils exploiting double-stranded serpentine design have been successfully applied as wireless, passive epidermal strain sensors.

Keywords: wearable, flexible electronics, epidermal, vital sign monitor, freeform manufacture

1. INTRODUCTION

Our body is radiating data about ourselves continuously and individually. Wearable devices that can pick up and transmit signals from the human body have the potential to transform mobile health (mHealth) and human-machine interface (HMI), which prompted the Forbes Magazine to name 2014 as the year of wearable technology [1]. However, since wafer-based integrated circuits are planar, rigid, and brittle, state-of-the-art wearable devices are mostly in the form factors of "chips on tapes" or "bricks on straps", which are unable to maintain intimate and prolonged contact with the curved, soft, and dynamic human body for long-term, high-fidelity physiological signal monitoring [2].

Recent advancements in flexible and stretchable electronics have provided viable solutions to bio-mimetic electronic skins [3-5] and bio-integrated electronics [6, 7]. Among many breakthroughs, epidermal electronic systems (EES) represents a paradigm-shift wearable device whose thickness and mechanical properties can match that of human epidermis [8]. As a result, the EES can conform to human skin like a temporary transfer tattoo and deform with the skin without detachment or fracture. The EES was first developed to monitor electrophysiological signals [8], and thereafter skin temperature [9, 10], skin hydration [11-13], sweat [14, 15], and even movement disorders [16]. Moreover, near field communication (NFC) antenna based on EES technology has also been reported [13, 15, 17].

The thinness and softness of EES, however, lead to collapsing and crumpling after it is peeled off human skin, making its use as a disposable electronic tattoo ideal. As a result, the success of EES hinges on the realization of low cost, high throughput manufacture. Current EES manufacture relies on standard microelectronics fabrication processes including vacuum deposition of films, spin coating, photolithography, wet and dry etching, as well as transfer-printing [8, 13, 17]. Although it has been proved effective, there are several limitations associated with such process: first, a rigid handle wafer has to be used for photolithography, making it incompatible with roll-to-roll process; second, the high cost associated with cleanroom facilities, photo masks, photolithography chemicals, and manpower prevents EES from being inexpensive and disposable; third, high vacuum film deposition is time consuming and hence impractical for thick films; fourth, the EES size is limited to the size of the handle wafer, which is limited by the smallest vacuum chamber throughout the process; and last but not least, the high manpower demand of the manufacturing process greatly limits the accessibility of EES.

Micro- and Nanotechnology Sensors, Systems, and Applications VIII, edited by Thomas George, Achyut K. Dutta, M. Saif Islam, Proc. of SPIE Vol. 9836, 98361B · © 2016 SPIE
CCC code: 0277-786X/16/$18 · doi: 10.1117/12.2224690

Our newly invented "cut-and-paste" method offers a very simple and immediate solution to the above mentioned challenges. Instead of doing high vacuum metal deposition, thin metal-on-polymer laminates of various thicknesses can be directly purchased from industrial manufacturers. Instead of using photolithography patterning, a benchtop electronic cutting machine is used to mechanically carve out the designed patterns, with excess being removed, which is a freeform, subtractive manufacturing process, inverse to the popular freeform, additive manufacturing technology [18]. The cutting

nanshulu@utexas.edu; phone 512-471-4208; fax 512-471-3788; https://lu.ae.utexas.edu/
machine can pattern on thin sheet metals and polymers up to 12 inches wide and several feet long, largely exceeding lab-scale wafer sizes. Since the patterns can be carved with the support of thermal release tapes (TRT), the patterned films can be directly printed onto a variety of tattoo adhesives and medical tapes with almost 100% yield. The whole process can be completed on an ordinary bench without any wet process within ten minutes, which allows rapid prototyping. Equipment used in this process only includes a desktop cutting machine for thin film patterning and a hot plate for TRT heating, which enables portable manufacture. Since no rigid handle wafer is needed throughout the process, the "cut-and-paste" method is intrinsically compatible with roll-to-roll manufacture. To demonstrate the "cut-and-paste" method, multimaterial epidermal sensor systems (ESS) are fabricated and applied to measure electrophysiological (EP) signals such as electrocardiogram (ECG), electromyogram (EMG), electroencephalogram (EEG), skin temperature, skin hydration, and respiratory rate. A planar stretchable coil of 9-μm-thick aluminum ribbons exploiting the double-stranded serpentine design is also integrated on the ESS as a low frequency, wireless strain gauge, which can also serve as NFC antenna in the future.

2. METHODS

A schematic of the benchtop "cut-and-paste" process is shown in Figure 1. Since stiff-polymer-supported blanket metal films are more stretchable than freestanding metal sheets [19], we always use metal-on-stiff-polymer laminates as the starting materials. Starting materials such as gold (Au) coated polyimide and aluminum (Al) coated polyethylene terephthalate (PET) are commonly used as thermal control or cable shielding laminates and can be purchased from industrial suppliers such as Sheldahl (Northfield, MN) and Neptco (Pawtucket, RI). We were able to purchase a small roll of 9-μm-thick Al on 12-μm-thick PET laminates from Neptco. Since only a small amount of polymer-supported Au foils are used in this research, we chose to use thermal evaporation to deposit several batches of 100-nm-thick Au films on 13-μm-thick transparent PET foils (Goodfellow, USA). To manufacture Au-based stretchable EP electrodes, resistance temperature detectors (RTD), and impedance sensors, the Au-on-PET foil was uniformly bonded to a flexible, single-sided TRT (Semiconductor Equipment Corp., USA) with Au side touching the adhesive of the TRT. The other side of the TRT was then adhered to a tacky flexible cutting mat, as shown in Figure 1a. The cutting mat was fed into an electronic cutting machine (Silhouette Cameo, USA) with the PET side facing the cutting blade. By importing our AutoCAD design into the Silhouette Studio software, the cutting machine can automatically carve the Au-on-PET sheet with designed seams within minutes (Figure 1b). Once seams were formed, the TRT was gently peeled off from the cutting mat (Figure 1c). Slightly baking the TRT on a 115 °C hotplate for 1~2 minutes deactivated the adhesives on the TRT so that the excesses can be easily peeled off by tweezers (Figure 1d), leaving only the EP electrodes, RTD, and impedance sensors loosely resting on the TRT. The patterned devices were finally printed onto a target substrate with native adhesives, which could be a temporary tattoo paper (Silhouette) or a medical tape, such as 3M Tegaderm™ transparent dressing or 3M kind removal silicone tape (KRST) (Figure 1e), yielding a Au-based ESS (Figure 1f). Steps illustrated by Figures 1a-e can be repeated for other thin sheets of metals and polymers, which can be printed on the same target substrate with alignment markers, rendering a multimaterial, multiparametric ESS ready for skin mounting.

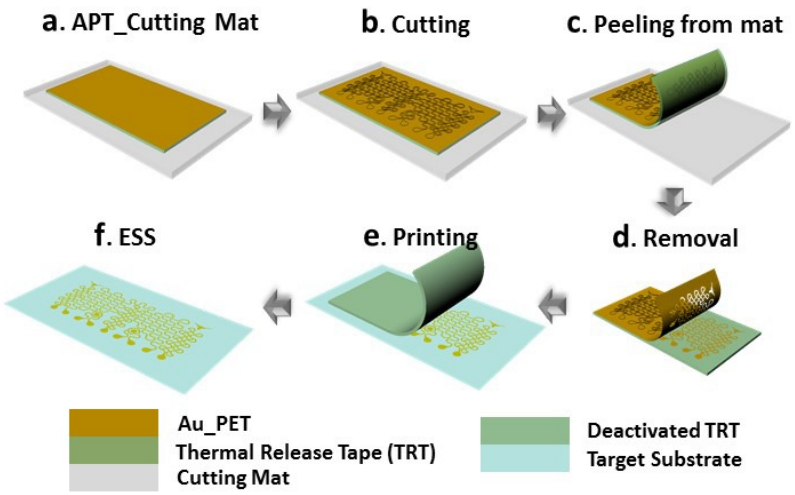

Figure 1. Schematics for the "cut-and-paste" process. (a) Au-PET-TRT (APT) laminated on the cutting mat with PET being the topmost layer. (b) Carving designed seams in the Au-PET layer by an automated mechanical cutting machine. (c) Peeling APT off the cutting mat. (d) Removing excessive Au-PET layer after deactivating the TRT on hot plate. (e) Printing patterned Au-PET layer onto target substrate. (f) Resulted epidermal sensor systems (ESS) with Au being the topmost layer.

A multimaterial, multiparametric ESS supported by transparent temporary tattoo paper and its white liner is shown in Figure 2a, which includes three Au-based filamentary serpentine (FS) EP electrodes, one Au-based FS RTD, two Au-based dot-ring impedance sensors, and an Al-based planar stretchable coil. In this picture, all Au-based sensors have the Au side facing up and in the future touching human skin as Au is a biocompatible metal. The stretchable coil, however, has the blue colored PET facing up because PET has demonstrated good biocompatibility [20] but some people's skin can be allergic to Al. For the three EP electrodes, the inter-electrode distance is set to be 2 cm for effective EP signal recording [21]. The FS is designed with a 1/5 ribbon width to arc radius ratio in order to balance the trade-off between stretchability and occupied area, according to our recent mechanics of serpentine research [22]. The same FS design is not applicable to the stretchable Al coil because it will consume too much space when more turns are needed for higher inductance. Therefore a double-stranded serpentine design is proposed (Figure 2a), which saves space without compromising the number of turns or the stretchability too much. The two longhorns at the upper left and right corners of the Au pattern serve as alignment markers for printing Au and Al devices on the same tape. The overall size of the device area is 7.5 cm × 5 cm.

The stretchability of different serpentine ribbons on Tegaderm tapes were tested using a customized tensile tester with *in situ* resistance measurement and top down webcam observation (Figure 2b left panel) [23]. When electrical resistance is measured as a function of the applied uniaxial tensile strain, the applied strain at which the resistance explodes (e.g. R/R_0 = 1.1) is considered the strain-to-rupture or stretchability [19]. According to Figure 2b right panel, while straight Al-on-PET and Au-on-PET ribbons exhibit limited stretchability (2.89% and 13.72%, respectively), their serpentine-shaped ribbons are much more stretchable, well beyond the elastic limit of human skin (30%) [24]. For serpentine ribbons such as the Al coil and Au RTD, rupture sites are always found at the crest of the arc whereas for serpentine network such as the Au EP electrode, fracture first occurs at ribbon intersections due to strain concentration and overcutting at turning points.

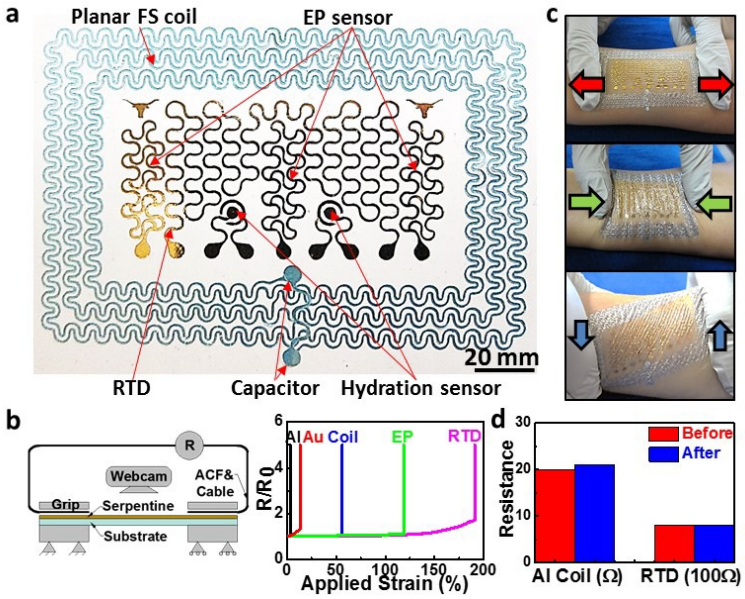

Figure 2. Multimaterial, multiparametric ESS. (a) Top view of an ESS which incorporates three electrophysiological (EP) electrodes (Au-PET), a resistance temperature detector (RTD) (Au-PET), two coaxial dot-ring impedance sensors (Au-PET), and a wireless planar stretchable strain sensing coil (Al-PET), all in filamentary serpentine (FS) layout. (b) Resistance change measured as function of applied strain. "Al" denotes straight Al-PET ribbon, "Au" denotes straight Au-PET ribbon, "Coil" denotes Al-PET serpentine ribbon used in wireless strain sensor coil, "EP" denotes Au-PET serpentine ribbon used in EP electrode, and "RTD" denotes Au-PET serpentine ribbon used in RTD. (c) ESS on human skin demonstrating excellent deformability during stretch (top), compression (middle), shear (bottom). (d) Resistance of Al coil and Au RTD before and after all possible deformations of skin-mounted ESS.

3. RESULTS

The multiparametric ESS has been successfully applied to perform continuous EP, skin temperature, and skin hydration measurements. EP signals on the surface of human skin measure the flow of ions in the underneath tissues and organs, which reflects their health and function. For example, noninvasive ambulatory monitoring of ECG on human chest can help detect multiple important features of heart malfunction like irregular heartbeat (arrhythmia) [25]. EMG reflects human muscle activity and can identify neuromuscular diseases and serve as a control signal for prosthetic devices or other machines [21]. EEG measured from the surface of human scalp can be used to not only capture cognitive and memory performance [26], but also chart brain disorders like epilepsy [27] and stroke [28]. Figure 3a displays ECG measurement from the human chest using silver/silver chloride (Ag/AgCl) gel electrodes and the ESS without applying any conductive gels. Both ESS and Ag/AgCl electrodes were connected to a small portable amplifier (AvatarEEG™) with a shared ground port through a homemade reusable connector. Out of the three EP electrodes integrated on the ESS, the center one is utilized as a ground and the other two electrodes measure EP signals in a bipolar montage to reflect the difference in electrical potential. Signals recorded by this amplifier were processed using a Principle Component Analysis based algorithm [40], with the final results shown in Figure 3a. It is evident that the important features of ECG are captured by both electrodes, but the ECG measured by our ESS demonstrates higher amplitude. We also placed the same type of ESS over the forearm, specifically on the flexor muscles, to measure the EMG during two hand clenches (Figure 3b). The intensity of the gripping force can be measured by a commercial dynamometer (Exacta™) and it is clear that the higher gripping force corresponds to higher signal amplitude in the measured EMG. Finally, we measured EEG by adhering Ag/AgCl electrodes and the ESS on human forehead. Both electrodes were referenced against one FS electrode placed behind the human ear on the mastoid location, as shown in Figure 3c left panel. Signals were high and low passed filtered at 0.1Hz and 40 Hz respectively. Frequency spectrums were calculated using standard fast Fourier transformations (FFT). Their FFT spectrums almost fully overlap in the upper right panel of Figure 3c, which confirms that conventional and ESS electrodes are almost indistinguishable in measured EEG signals, but the ESS offers additional merits including conformability, softness and customizable electrode patterns. The lower right panel of Figure

3c compares the FFT of the ESS measured EEG signal while the participant maintained eyes open and eyes closed. One can note the expected increase in relative alpha power associated with the eyes closed period relative to eyes open (centered around 10 Hz).

In addition to EP, skin temperature, skin hydration, and skin deformation are also useful indicators of human physiology. For example, skin temperature is associated with cardiovascular health, cognitive state, and tumor malignancy [29-31]. Skin hydration is widely used in dermatology and cosmetology for the detection of diseases (e.g., eczema, atopic dermatitis, etc.) [32, 33], the assessment of mental stress or hormone levels [34, 35], and the evaluation of medical therapies or cosmetic treatments [36, 37]. Quantifying skin deformation is useful for the detection of gesture [38], respiration, as well as motion disorders [16]. Ultrathin, stretchable RTD can be built as a narrow but long ribbon of Au FS as labeled in Figure 2a, which has a high initial resistance R_0 and a predictable change in resistance as the temperature changes. To perform skin temperature measurement, the epidermal RTD was attached on human forearm, along with a commercial thermocouple (TMD-56, Amprobe) as pictured in Figure 3d left panel. Skin temperature measured by the epidermal RTD and the thermocouple are plotted in Figure 3d right panel. Skin temperature was initially stabilized at around 30 °C. At t = 2'13", an ice bag was brought in contact with the RTD and skin for 1 minute and then removed. The corresponding temperature drop and recovery are clearly visible in the graph of Figure 3d. The strong correlation between RTD and thermocouple outputs has validated the use of RTD as a soft and stretchable skin temperature detector.

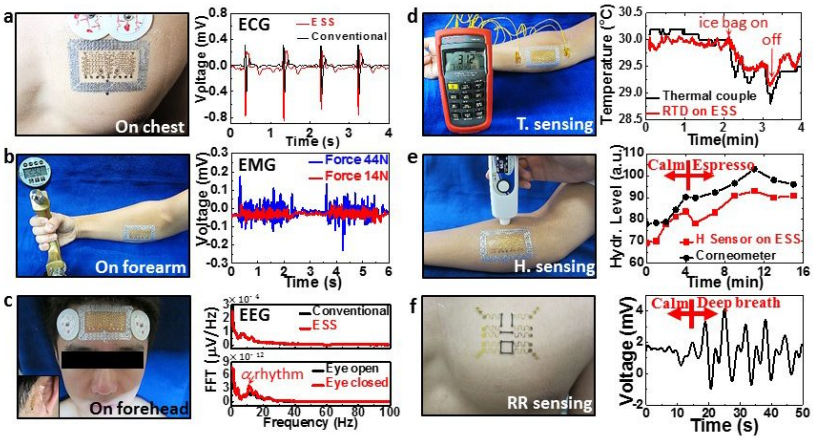

Figure 3. ECG, EMG, EEG, skin temperature, skin hydration, and respiratory rate measurements by ESS. (a) ECG simultaneously measured by ESS (red) and Ag/AgCl electrodes (black). Stronger ECG signals were obtained by the ESS. (b) ESS attached on human forearm for EMG measurement when the subject is gripping a commercial dynamometer with different forces. Higher amplitude corresponds to higher gripping force. (c) EEG measured on human forehead by both ESS and Ag/AgCl electrodes. Two frequency spectrum of the EEG are well overlapped. 10 Hz alpha rhythm measured by ESS is clearly visible when eyes were closed. (d) Skin temperature changes measured by both epidermal RTD and thermocouple found good correlation. (e) Real time skin hydration before and after Espresso intake measured by both commercial coaxial corneometer and ESS. (f) Voltage outputs from the ECR Wheatstone bridge during normal and deep breath.

Skin hydration level is reflected by the impedance of skin [11], which can be conveniently measured by impedance sensors in the coaxial dot-ring design as labeled in Figure 2a. Laminating the epidermal hydration sensor (H. sensor) on human skin, an inductance, capacitance, and resistance (LCR) meter (Digital Multimeter, Rigol) was used to measure the impedance at different frequencies as well as different skin hydration levels. A commercial corneometer (MoistureMeterSC Compact, Delfin Inc.) was used to quantify the skin hydration level. Figure 3e illustrates a continuous hydration measurement with both epidermal H. sensor and the corneometer before and after the subject drank a can of cold Espresso. The caffeine in Espresso is expected to lead to perspiration as it stimulates human central nervous system, which activates the sweat glands. The results are shown in Figure 3e right panel, which clearly indicates gradual increase of hydration after drinking Espresso based on the measurements of both the epidermal H. sensor and the corneometer. The initial increase in hydration before drinking Espresso is believed to be caused by the ESS lamination. It is also interesting to note that skin hydration peaked seven minutes after drinking the Espresso and started to decay after that, likely due to the thermoregulation of the body. An artifact of contact pressure in measuring skin hydration with ESS was noticed.

Epidermal respiratory rate sensor was build using electrically conductive rubber (ECR), which is similar to our previous soft strain gauge work [39], but is made by the more cost and time effective "cut-and-paste" method. Unlike conventional micro-fabrication techniques that are limited to inorganic materials, the "cut-and-paste" process developed here can be applied to a much broader category of materials, including elastomeric sheets. As a demonstration, we fabricated stretchable strain gauges employing ECR (Elastosil LR 3162, Wacker Silicones) as the strain-sensitive resistor, and Au-on-PET serpentine ribbons as the stretchable interconnects. On skin test was performed by applying Tegaderm-supported ECR-based strain gauges on the chest of a human subject (Figure 3f left picture) and various respirational patterns were studied. Figure 3f right graph illustrates the deformation of human chest during normal breath and deep breath using the Wheatstone bridge. Larger amplitude and lower frequency are observed for deep breath.

Compared with silicon nanomembrane [38, 40] and ECR [39] based skin-integrated stretchable strain gauges, epidermal strain sensors based on planar stretchable capacitor can operate wirelessly [13]. Instead of using stretchable capacitor, here we explore planar stretchable inductors to build wireless epidermal strain sensors. The double stranded serpentine design of the planar inductor coil as depicted in Figure 2a has taken into account overall size, stretchability, overall inductance, and inductance sensitivity to strain. Figure 4 illustrates the wireless measurement on the sensor coil. A circular reader coil is connected to an Impedance Analyzer (HP 4194A) via a standard BNC-RCA adaptor. The reader is inductively coupled to the sensor coil in a transformer like configuration (Figure 4a). The experimental setup is given in Figure 4b and there was no cable connection between the reader and the sensor coil. By measuring the impedance response of the coupled circuit as a function of frequency, the resonance frequency corresponds to a dip in the phase-frequency curve.

We performed uniaxial stretch tests on Tegaderm supported stretchable coils (Figure 4c) and recorded strain-induced shift of resonance frequency of the coupled circuit, as shown in Figure 4d. Measured resonance frequency as a function of applied strain is plotted in red in Figure 4e, which shows a monotonic decay as the sensor coil is uniaxially elongated. The resonance frequency shifted from 38.6 MHz in the undeformed shape down to 34.3 MHz at the strain of 20%, which is more sensitive to deformation compared to a previously reported stretchable epidermal antenna [17].

FEM analysis on stretchable coils has been carried out through a combination of ABAQUS standard and ANSYS Maxwell package and the results are plotted in blue in Figure 4e, with squares representing serpentine coils and triangles representing straight coils. Comparing the two results, straight coil appears less sensitive to applied strain, which is undesirable for strain sensing application but could be advantageous for antenna application when stable resonance frequency is needed. Analytical modeling of single and multi-turn straight coils are given in Figure S20. All results (experimental, numerical, and analytical) suggest a decay of resonance frequency as the tensile strain enlarges, but the discrepancy between experimental and FEM results requires future studies.

The effect of distance (coupling factor k as labeled in Figure 4a) between the reader and the sensor coils has also been investigated. It is found that the resonance frequency does not depend on the distance whereas the phase dip does. Specifically, the smaller the gap, the larger the phase dip, thus the higher coupling factor. One way to improve the coupling factor and hence enlarge the sensing distance is to increase the overall size of either the reader or the sensor coil, with a tradeoff in the wearability of the sensor and the portability of the reader.

The skin deformation measurement was performed by attaching the sensor coil on the dorsal wrist and bringing the reader coil within 45 mm distance from the sensor coil. 3 layers of tattoo paper (Silhouette) were applied between the sensor coil and the skin to compensate for capacitive loading induced by the skin. Three wrist gestures "flat", "stretch", and "compress" were measured (Figure 4f). Phase measurement for the three gestures are plotted in Figure 4g, which reveals several interesting findings. First, the resonance frequency drops from 38.6 MHz to 13.92 MHz before and after the sensor coil was applied on the skin, which is due to the substantial capacitive loading induced by the skin [41]. The second observation is that "stretch" reduces the resonance frequency (from 13.92 MHz to 12.99 MHz) whereas "compress" slightly increases resonance frequency (from 13.92 MHz to 14.41 MHz), as expected. Repeatability test was conducted by repeating the wrist gestures in the sequence "flat", "stretch", "compress" twice and the result shows that the wireless strain gauge coil can offer very repeatable measurements of joint bending.

The planar stretchable coil also has the potential to work as an NFC antenna for transferring the local signals measured by the ESS wirelessly to a remote receiver [17]. In order to transfer data properly, the resonance frequency should stay as steady as possible during the transferring process. We therefore tested the coil response when it is placed on human chest and the subject was under deep inhalation and exhalation. It is found that the resonance frequency only changed from 13.06 MHz to 12.80 MHz, for either deep inhalation or exhalation. The insensitivity of resonance frequency to chest

deformation associated inhalation and exhalation makes it possible to be used as a stable epidermal antenna for chest ESS.

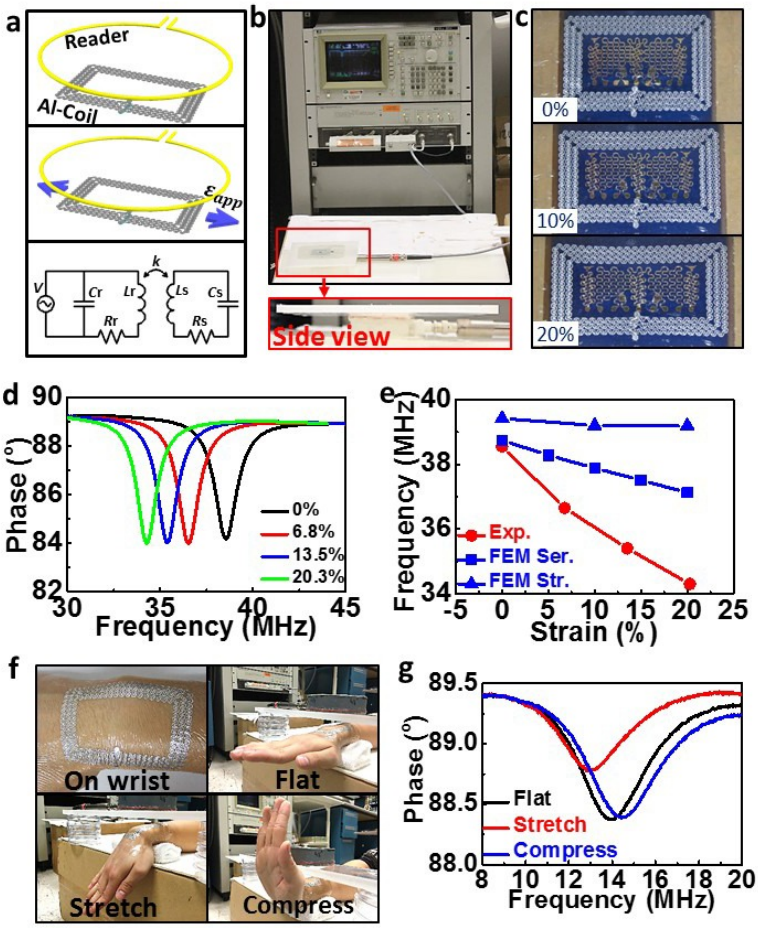

Figure 4. Wireless epidermal strain sensor based on stretchable Al coil. (a) Schematics of the wirelessly coupled reader and sensor coils. (b) Experimental setup for the measurement of the resonance frequency of the coupled system. The sensor coil was place on top of the reader coil and separated by a 6 mm thick acrylic slab plus 4 mm air gap. The reader was connected to an Impedance Analyzer (HP 4194A). (c) Images of the sensor coil stretched horizontally by 0%, 10% and 20%, respectively. (d) Phase response of the coupled system as a function of sweeping frequency at different applied strains. (e) Both experimental (red) and FEM (blue) results showing decreased resonance frequency with increased tensile strain. (f) Sensor coil attached on human wrist (top left) under different hand gestures: "flat" (top right), "stretch" (bottom left) and "compress" (bottom right). (g) Resonance frequency decreases when the sensor coil is stretched by the wrist, and increases when compressed by the wrist.

4. CONCLUSIONS

In conclusion, we have demonstrated a versatile, cost and time effective method to manufacture multimaterial, multiparametric ESS that can be intimately but noninvasively and unobstructively applied on human skin to measure ECG, EMG, EEG, skin temperature, skin hydration, respiratory rate, and joint bending. The "cut-and-paste" method enables completely dry, benchtop, freeform, and portable manufacture of ESS within minutes, without using any vacuum facilities or chemicals. The "cut-and-paste" method has proved effective in patterning metal-on-polymer laminates and elastomeric sheets, but it is not applicable to ceramic-coated polymer as indentation of the cutting blade would easily fracture intrinsically brittle ceramic film. However, we have demonstrated a variation of the "cut-and-paste" method to manufacture highly stretchable transparent interconnects based on brittle indium tin oxide (ITO) film [23]. In addition to ESS, the "cut-and-paste" manufacturing method is expected to be useful for the manufacture of other stretchable devices

including stretchable circuit boards which house rigid IC chips [42] and deployable structure health monitoring sensor networks [43].

ACKNOWLEDGEMENTS

This work is based upon work supported in part by the National Science Foundation under grant Nos. CMMI-1301335 and CMMI-1351875. N.L. acknowledges the 3M Non-Tenured Faculty Award. Any opinions, findings and conclusions or recommendations expressed in this material are those of the authors and do not necessarily reflect the views of the National Science Foundation nor 3M.

REFERENCE

[1] Bowden, N., Brittain, S., Evans, A. G., Hutchinson, J. W. and Whitesides, G. M., "Spontaneous formation of ordered structures in thin films of metals supported on an elastomeric polymer", Nature 393, 146 (1998).
[2] Ives, J. R., Mirsattari, S. M. and Jones, D., "Miniaturized, on-head, invasive electrode connector integrated EEG data acquisition system", Clin Neurophysiol 118, 1633 (2007).
[3] Schwartz, G., Tee, B. C. K., Mei, J. G., Appleton, A. L., Kim, D. H., Wang, H. L. and Bao, Z. N., "Flexible polymer transistors with high pressure sensitivity for application in electronic skin and health monitoring", Nat Commun 4, 1859 (2013).
[4] Gong, S., Schwalb, W., Wang, Y. W., Chen, Y., Tang, Y., Si, J., Shirinzadeh, B. and Cheng, W. L., "A wearable and highly sensitive pressure sensor with ultrathin gold nanowires", Nat Commun 5, 3132 (2014).
[5] Gong, S., Lai, D. T. H., Su, B., Si, K. J., Ma, Z., Yap, L. W., Guo, P. and Cheng, W., "Highly Stretchy Black Gold E-Skin Nanopatches as Highly Sensitive Wearable Biomedical Sensors", Advanced Electronic Materials 1, 1 (2015).
[6] Kim, D. H., Ghaffari, R., Lu, N. S. and Rogers, J. A., "Flexible and Stretchable Electronics for Bio-Integrated Devices", Annual review of biomedical engineering 14, 113 (2012).
[7] Yeo, W. H., Webb, R. C., Lee, W., Jung, S. and Rogers, J. A., "Bio-integrated electronics and sensor systems", Micro- and Nanotechnology Sensors, Systems, and Applications V 8725, (2013).
[8] Kim, D. H., Lu, N. S., Ma, R., Kim, Y. S., Kim, R. H., Wang, S. D., Wu, J., Won, S. M., Tao, H., Islam, A., Yu, K. J., Kim, T. I., Chowdhury, R., Ying, M., Xu, L. Z., Li, M., Chung, H. J., Keum, H., McCormick, M., Liu, P., Zhang, Y. W., Omenetto, F. G., Huang, Y. G., Coleman, T. and Rogers, J. A., "Epidermal Electronics", Science 333, 838 (2011).
[9] Feng, X., Yang, B. D., Liu, Y. M., Wang, Y., Dagdeviren, C., Liu, Z. J., Carlson, A., Li, J. Y., Huang, Y. G. and Rogers, J. A., "Stretchable Ferroelectric Nanoribbons with Wavy Configurations on Elastomeric Substrates", Acs Nano 5, 3326 (2011).
[10] Hattori, Y., Falgout, L., Lee, W., Jung, S. Y., Poon, E., Lee, J. W., Na, I., Geisler, A., Sadhwani, D., Zhang, Y. H., Su, Y. W., Wang, X. Q., Liu, Z. J., Xia, J., Cheng, H. Y., Webb, R. C., Bonifas, A. P., Won, P., Jeong, J. W., Jang, K. I., Song, Y. M., Nardone, B., Nodzenski, M., Fan, J. A., Huang, Y. G., West, D. P., Paller, A. S., Alam, M., Yeo, W. H. and Rogers, J. A., "Multifunctional Skin-Like Electronics for Quantitative, Clinical Monitoring of Cutaneous Wound Healing", Adv Healthc Mater 3, 1597 (2014).
[11] Huang, X., Yeo, W. H., Liu, Y. H. and Rogers, J. A., "Epidermal Differential Impedance Sensor for Conformal Skin Hydration Monitoring", Biointerphases 7, 1 (2012).
[12] Huang, X., Cheng, H., Chen, K., Zhang, Y., Zhang, Y., Liu, Y., Zhu, C., Ouyang, S.-c., Kong, G.-W., Yu, C., Huang, Y. and Rogers, J. A., "Epidermal Impedance Sensing Sheets for Precision Hydration Assessment and Spatial Mapping", Biomedical Engineering, IEEE Transactions on 60, 2848 (2013).
[13] Lu, N. and Kim, D. H., "Flexible and stretchable electronics paving the way for soft robotics", Soft Robotics 1, 53 (2013).
[14] Bandodkar, A. J., Molinnus, D., Mirza, O., Guinovart, T., Windmiller, J. R., Valdes-Ramirez, G., Andrade, F. J., Schoning, M. J. and Wang, J., "Epidermal tattoo potentiometric sodium sensors with wireless signal transduction for continuous non-invasive sweat monitoring", Biosens Bioelectron 54, 603 (2014).
[15] Huang, X., Liu, Y. H., Chen, K. L., Shin, W. J., Lu, C. J., Kong, G. W., Patnaik, D., Lee, S. H., Cortes, J. F. and Rogers, J. A., "Stretchable, Wireless Sensors and Functional Substrates for Epidermal Characterization of Sweat", Small 10, 3083 (2014).

[16] Son, D., Lee, J., Qiao, S., Ghaffari, R., Kim, J., Lee, J. E., Song, C., Kim, S. J., Lee, D. J., Jun, S. W., Yang, S., Park, M., Shin, J., Do, K., Lee, M., Kang, K., Hwang, C. S., Lu, N. S., Hyeon, T. and Kim, D. H., "Multifunctional wearable devices for diagnosis and therapy of movement disorders", Nat Nanotechnol 9, 397 (2014).
[17] Kim, J., Banks, A., Cheng, H., Xie, Z., Xu, S., Jang, K.-I., Lee, J. W., Liu, Z., Gutruf, P., Huang, X., Wei, P., Liu, F., Li, K., Dalal, M., Ghaffari, R., Feng, X., Huang, Y., Gupta, S., Paik, U. and Rogers, J. A., "Epidermal Electronics with Advanced Capabilities in Near-Field Communication", Small, n/a (2014).
[18] Pacheco, M. A. and Marshall, C. L., "Review of dimethyl carbonate (DMC) manufacture and its characteristics as a fuel additive", Energ Fuel 11, 2 (1997).
[19] Lu, N. S., Wang, X., Suo, Z. and Vlassak, J., "Metal films on polymer substrates stretched beyond 50%", Appl Phys Lett 91, 221909 (2007).
[20] Seitz, H., Marlovits, S., Schwendenwein, I., Muller, E. and Vecsei, V., "Biocompatibility of polyethylene terephthalate (Trevira (R) hochfest) augmentation device in repair of the anterior cruciate ligament", Biomaterials 19, 189 (1998).
[21] Valdivia, V., Barrado, A., Lazaro, A., Zumel, P. and Raga, C., "Easy Modeling and Identification Procedure for "Black Box" Behavioral Models of Power Electronics Converters with Reduced Order Based on Transient Response Analysis", Apec: 2009 Ieee Applied Power Electronics Conference and Exposition, Vols 1- 4, 318 (2009).
[22] Widlund, T., Yang, S., Hsu, Y.-Y. and Lu, N., "Stretchability and compliance of freestanding serpentine-shaped ribbons", Int J Solids Struct 51, 4026 (2014).
[23] Yang, S., Ng, E. and Lu, N., "Indium Tin Oxide (ITO) Serpentine Ribbons on Soft Substrates Stretched beyond 100%", Extreme Mechanics Letters 2, 37 (2015).
[24] Arumugam, V., Naresh, M. D. and Sanjeevi, R., "Effect of Strain-Rate on the Fracture-Behavior of Skin", J Bioscience 19, 307 (1994).
[25] Thakor, N. V. and Zhu, Y. S., "Applications of Adaptive Filtering to Ecg Analysis - Noise Cancellation and Arrhythmia Detection", Ieee T Bio-Med Eng 38, 785 (1991).
[26] Klimesch, W., "EEG alpha and theta oscillations reflect cognitive and memory performance: a review and analysis", Brain Res Rev 29, 169 (1999).
[27] Rosenow, F., Klein, K. M. and Hamer, H. M., "Non-invasive EEG evaluation in epilepsy diagnosis", Expert review of neurotherapeutics 15, 425 (2015).
[28] Jordan, K. G., "Emergency EEG and continuous EEG monitoring in acute ischemic stroke", J Clin Neurophysiol 21, 341 (2004).
[29] Wyss, C. R., Brengelm.Gl, Johnson, J. M., Rowell, L. B. and Niederbe.M, "Control of Skin Blood-Flow, Sweating, and Heart-Rate - Role of Skin Vs - Core Temperature", J Appl Physiol 36, 726 (1974).
[30] Makinen, T. M., Palinkas, L. A., Reeves, D. L., Paakkonen, T., Rintamaki, H., Leppaluoto, J. and Hassi, J., "Effect of repeated exposures to cold on cognitive performance in humans", Physiol Behav 87, 166 (2006).
[31] Ng, E. Y. K., "A review of thermography as promising non-invasive detection modality for breast tumor", Int J Therm Sci 48, 849 (2009).
[32] Blichmann, C. and Serup, J., "Hydration Studies on Scaly Hand Eczema", Contact Dermatitis 16, 155 (1987).
[33] Hon, K. L. E., Wong, K. Y., Leung, T. F., Chow, C. M. and Ng, P. C., "Comparison of skin hydration evaluation sites and correlations among skin hydration, transepidermal water loss, SCORAD index, Nottingham eczema severity score, and quality of life in patients with atopic dermatitis", Am J Clin Dermatol 9, 45 (2008).
[34] Sator, P. G., Schmidt, J. B., Rabe, T. and Zouboulis, C. C., "Skin aging and sex hormones in women - clinical perspectives for intervention by hormone replacement therapy", Exp Dermatol 13, 36 (2004).
[35] Tran, B. W., Papoiu, A. D. P., Russoniello, C. V., Wang, H., Patel, T. S., Chan, Y. H. and Yosipovitch, G., "Effect of Itch, Scratching and Mental Stress on Autonomic Nervous System Function in Atopic Dermatitis", Acta Derm-Venereol 90, 354 (2010).
[36] Kleiner, S. M., "Water: An essential but overlooked nutrient", J Am Diet Assoc 99, 200 (1999).
[37] Boguniewicz, M., Nicol, N., Kelsay, K. and Leung, D. Y. M., "A multidisciplinary approach to evaluation and treatment of atopic dermatitis", Semin Cutan Med Surg 27, 115 (2008).
[38] Ying, M., Bonifas, A. P., Lu, N. S., Su, Y. W., Li, R., Cheng, H. Y., Ameen, A., Huang, Y. G. and Rogers, J. A., "Silicon nanomembranes for fingertip electronics", Nanotechnology 23, 344004 (2012).
[39] Kandasamy, R., Wang, X. Q. and Mujumdar, A. S., "Transient cooling of electronics using phase change material (PCM)-based heat sinks", Appl Therm Eng 28, 1047 (2008).
[40] Kim, D. H., Ghaffari, R., Lu, N. S., Wang, S. D., Lee, S. P., Keum, H., D'Angelo, R., Klinker, L., Su, Y. W., Lu, C. F., Kim, Y. S., Ameen, A., Li, Y. H., Zhang, Y. H., de Graff, B., Hsu, Y. Y., Liu, Z. J., Ruskin, J., Xu, L. Z., Lu, C.,

Omenetto, F. G., Huang, Y. G., Mansour, M., Slepian, M. J. and Rogers, J. A., "Electronic sensor and actuator webs for large-area complex geometry cardiac mapping and therapy", P Natl Acad Sci USA 109, 19910 (2012).
[41] Kinnen, E., "Electrical impedance of human skin.pdf", Medical electronics and biological engineering 3, 67 (1965).
[42] Xu, S., Zhang, Y. H., Jia, L., Mathewson, K. E., Jang, K. I., Kim, J., Fu, H. R., Huang, X., Chava, P., Wang, R. H., Bhole, S., Wang, L. Z., Na, Y. J., Guan, Y., Flavin, M., Han, Z. S., Huang, Y. G. and Rogers, J. A., "Soft Microfluidic Assemblies of Sensors, Circuits, and Radios for the Skin", Science 344, 70 (2014).
[43] Lanzara, G., Salowitz, N., Guo, Z. Q. and Chang, F. K., "A Spider-Web-Like Highly Expandable Sensor Network for Multifunctional Materials", Adv Mater 22, 4643 (2010).